Available online at www.sciencedirect.com
ScienceDirect
Bioorganic & Medicinal Chemistry 14 (2006) 8495–8505
Bioorganic & Medicinal Chemistry

Modification at the C9 position of the marine natural product isoaaptamine and the impact on HIV-1, mycobacterial, and tumor cell activity

Waseem Gul,[a] Nicholas L. Hammond,[a] Muhammad Yousaf,[a] John J. Bowling,[a] Raymond F. Schinazi,[b] Susan S. Wirtz,[b] Garcia de Castro Andrews,[c] Carmen Cuevas[c] and Mark T. Hamann[a,*]

[a]*Department of Pharmacognosy and the National Center for Natural Products Research (NCNPR), University of Mississippi School of Pharmacy, MS 38677, USA*
[b]*Department of Pediatrics, Emory University/VA Medical Center, Decatur Georgia 30033, USA*
[c]*Research & Development, PharmaMar S.A., 28770-Colmenar Viejo, Madrid, Spain*

Received 23 February 2006; revised 24 August 2006; accepted 28 August 2006
Available online 11 October 2006

Abstract—As part of an investigation to generate optimized drug leads from marine natural pharmacophores for the treatment of neoplastic and infectious diseases, a series of novel isoaaptamine analogs were prepared by coupling acyl halides to the C9 position of isoaaptamine (**2**) isolated from the *Aaptos* sponge. This library of new semisynthetic products was evaluated for biological activity against HIV-1, Mtb, AIDS-OI, tropical parasitic diseases, and cancer. Compound **4** showed potent activity against HIV-1 (EC_{50} 0.47 μg/mL), compound **19** proved to possess remarkable activity against *Mycobacterium intracellulare* with an IC_{50} and MIC value of 0.15 and 0.31 μg/mL, while compounds **4** and **17** possessed anti-leishmanial activity with IC_{50} values of 0.1 and 0.4 μg/mL, respectively. Compounds **16** and **17** showed antimalarial activity with EC_{50} values of 230 and 240 ng/mL, respectively, and compound **14** exhibited an EC_{50} of 0.05 μM against the Leukemia cell line K-562.

1. Introduction

The development of resistance and the toxicity associated with current chemotherapeutic agents has led to an increasing failure of existing drugs utilized in the treatment of various microbial, viral, and neoplastic disorders. The marine environment, and the unique natural products contained therein, remains a relatively untapped source of possibilities for novel drug development. As seen in Figure 1, the marine natural product aaptamine (**1**), first isolated by Nakamura,[1] has been reported to have antineoplastic and α-adrenoceptor blocking activity.[1,2] The closely related compound isoaaptamine (**2**) was first isolated by Fedoreev[3] from a sponge in the genus *Suberites* and later by two other groups from the sponge *Aaptos aaptos*.[4,5] Recently, isoaaptamine (**2**) was isolated from a sponge belonging to the genus *Hymeniacidon*.[6] Isoaaptamine (**2**) has also been reported to be a PKC inhibitor.[7] However, the recent investigation by Pettit et al. of PKC inhibition and tubulin polymerization showed only minimal activity.[8] However, further investigation by this group revealed that inhibition of the S-Phase of the cell cycle may be involved in the observed cytotoxicity which suggests a possible interaction with DNA or topoisomerase. The closely related bis(naphthalimide) derivative DMP 840 (**A**) has been reported to be a topoisomerase II inhibitor[9] and is currently undergoing phase I clinical trials.[10] Additionally, the analog LU 79553 (**B**) has shown efficacy in vivo against tumor xenographs.[11] The related acridine anticancer agent AAC (**C**) has also been shown to elicit its activity through modulation of topoisomerase II.[12–14] Additional SAR investigation suggests a positive correlation between nonelectrostatic binding free energy and anti-cancer potency of acridine derivatives.[15]

Aaptamine, isoaaptamine, and demethylated aaptamine have shown antifouling activity in the zebra mussel

Keywords: Isoaaptamine derivatives; Anti-cancer leads; Anti-HIV-1 activity; Marine natural products.
* Corresponding author. Tel.: +1 662 915 5730; fax: +1 662 916 6975; e-mail: mthamann@olemiss.edu

0968-0896/$ - see front matter © 2006 Elsevier Ltd. All rights reserved.
doi:10.1016/j.bmc.2006.08.042

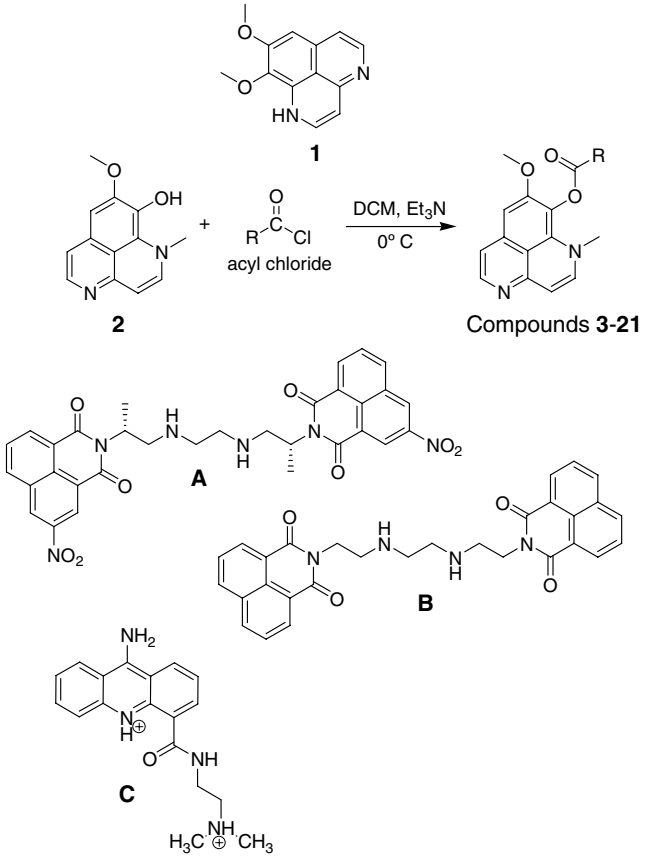

Figure 1. Aaptamine related structures.

assay with EC_{50} values of 24.2, 11.6, and 18.6 μM respectively.[16] Isoaaptamine (**2**) has shown activity against the protozoan that causes malaria, *Plasmodium falciparum*, with an IC_{50} of 1.8 and 0.6 μg/mL for the D6 and W2 clones, respectively. Pettit et al. recently reported dibenzyl aaptamine derivatives with activity against *Mycobacterium tuberculosis*.[17] Isoaaptamine has been shown to exhibit remarkable activity against cancer cell lines including P-338[4,6,8] (murine lymphocytic leukemia), KB16 (human mouth epidermoid carcinoma), A549 (human lung adenocarcinoma), and HT-29 (human colon adenocarcinoma).[4] The synthesis of aaptamine[18] (**1**) and isoaaptamine[19] (**2**) has recently been reported. The first SAR study of these compounds by Shen et al.[20] concluded that the C-9 hydroxyl position was important for cytotoxic activity and acylation causes a decrease in activity. Recently, the studies by Pettit et al.[6,8,17] with modifications at the hydroxyl and nitrogen positions of aaptamine have aided to further elucidate the SAR of these unique compounds. Specifically, para substituted phenyl substituents at one or both of the nitrogen positions increased activity.

In order to further investigate the SAR of side-chain attachment at the C9 hydroxyl position of isoaaptamine (**2**), which is readily available from the sponge *Aaptos* sp. in gram quantities, a series of analogs was generated. Presented here are 19 derivatives (Table 1) of isoaaptamine (**2**) generated with various acyl halides coupled at the C9 position of isoaaptamine (**2**) and their biological

Table 1. Isoaaptamine derivatives

Entry	Product	Yield (%)
3	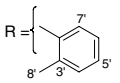	89
4	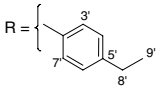	91
5	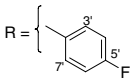	85
6	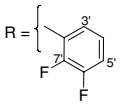	85
7	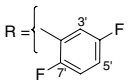	84
8	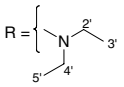	91
9	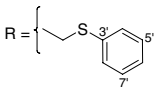	90
10	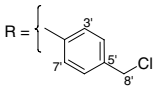	92
11	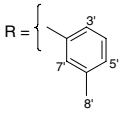	94
12	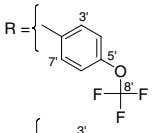	82
13	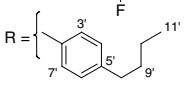	93
14	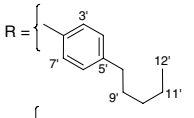	94
15	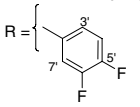	83
16	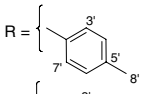	93
17	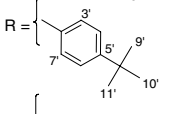	92
18	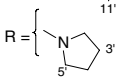	89
19	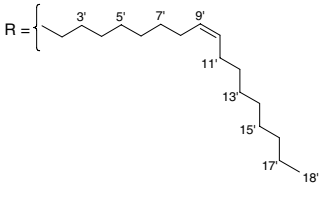	94

Table 1 (*continued*)

Entry	Product	Yield (%)
20	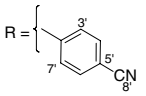	86
21	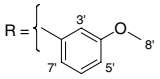	91

activity against a number of pathogens and cancer cell lines.

2. Results and discussion

The products **3**–**21** have been evaluated for activity against malaria, AIDS-OI pathogens, leishmania, cancer, HIV-1, and Mtb. The results from the in vitro assays and preliminary SAR are presented in Tables 2–4.

2.1. Anti-HIV-1

The anti-HIV-1 activity of isoaaptamine (**2**, 0.6 μM) and aaptamine (1.30 μM) has previously been reported.[21] The structure–activity relationship of fluorine substitution on an indole heterocyclic system has recently been reported to increase the potency of anti-HIV-1 activity.[22] Compounds **5**, **6**, **7**, and **15** contained fluorine at different positions on the phenyl substituent. Substitution of fluorine at the ortho position (**7**, EC_{50} 2.1 μg/mL), relative to substitution at other positions on the ring, increased activity except where there was adjacent fluorine (**6**, EC_{50} 37.7 μg/mL) in the meta position. Substitution of fluorine in the para position (**5**, EC_{50} 10.9 μg/mL; **15**, EC_{50} 16.6 μg/mL) was not as dramatic except where the substituent was a tri-fluorinated *O*-methyl group (**12**, EC_{50} 2.3 μg/mL). The position of fluorine substitution on the phenyl ring appears to be the most important aspect for anti-HIV-1 activity. Methyl substitution at the ortho, para, and meta positions (**3**, **11**, and **16**) reflects the same pattern seen in the fluorinated derivatives with highest activity in ortho (**3**, EC_{50} 1.3 μg/mL) substitution. Substitution at the para position with carbon chains of varying length shows a dramatic increase in activity with ethyl (**4**, EC_{50} 0.47 μg/mL) having better activity than methyl (**16**, EC_{50} 9.2 μg/mL) and a decrease as the chain is lengthened (**13**, EC_{50} 3.8 μg/mL; **14**, EC_{50} 18.8 μg/mL). Taking these results into consideration, short chain para substitution provides the best structure for anti-HIV-1 activity in this series of compounds.

2.2. AIDS opportunistic pathogens

Isoaaptamine (**2**) alone did not show toxic activity ($IC_{50} \leqslant 15$ μg/mL) against any of the tested microbes. However, several derivatives (**4**, **13**, **14**, and **17**) showed significant activity against *Mycobacterium intracellulare* with alkyl para substitution on the phenyl ring being the dominant pattern. Most interesting was the remarkable activity of compound **19** (IC_{50} 0.2 μg/mL, MIC 0.3 μg/mL) against *M. intracellulare* being more active than ciprofloxacin (IC_{50} 0.3 μg/mL, MIC 1.3 μg/mL).

Table 2. Anti-microbial activity data

Compound	IC_{50}/MIC						
	Candida albicans	*Cryptococcus neoformans*	*Staphylococcus aureus*	Methicillin resistant *Staphylococcus*	*Pseudomonas aeruginosa*	*Mycobacterium intracellulare*	*Aspergillus fumigatus*
2	—	—	—	—	—	—	—
3	—	15/20	—	—	—	5.0/10	—
4	10/20	5.5/10	8.0/20	8.0/20	—	0.8/2.5	—
5	—	—	—	—	—	3.5/10	—
6	—	—	—	—	—	—	—
7	—	—	—	—	—	—	—
8	—	—	—	—	—	—	—
9	—	—	—	—	—	—	—
10	—	—	6.5/20	6.5/20	—	5.0/10	—
11	—	15/20	—	—	—	4.0/10	—
12	—	6.5/10	—	—	—	1.0/5.0	—
13	3.0/5.0	1.5/2.5	1.5/2.5	1.5/2.5	—	0.5/1.3	5
14	4.5/10	3.0/5.0	3.0/5.0	3.0/5.0	—	1.0/2.5	10.0
15	—	—	—	—	—	5.5/20	—
16	—	10/20	—	—	—	1.0/5.0	—
17	6.5/10	1.5/2.5	3.0/5.0	2.5/5.0	—	0.5/1.3	10.0
18	—	—	—	—	—	—	—
19	—	—	—	—	—	0.2/0.3	—
20	—	—	10/20	10/20	—	—	—
21	—	—	—	—	—	10/20	—
Amphotericin B	0.3/1.3	0.6/2.5	—	—	—	—	—
Ciprofloxacin			0.1/0.6	0.1/0.6	0.1/1.3	0.3/1.3	—

IC_{50} is the concentration (μg/mL) that affords 50% inhibition of growth. $IC_{50} \leqslant 15$ μg/mL is considered active. For compounds that were considered active ($\leqslant$15 μg/mL), a MIC (minimum inhibitory concentration (μg/mL); lowest tested concentration that allows no detectable growth) was calculated. The screens were run at concentrations of 50, 10, and 2 μg/mL.

Table 3. Anti-Mtb, anti-HIV-1, anti-malarial, and anti-leishmania data

Compound	*Mycobacterium tuberculosis* (H37Rv) MIC (μg/mL)	*P. falciparum* (D6 clone) IC_{50} (μg/mL)	*P. falciparum* (chloroquine-resistant W2 clone) IC_{50} (μg/mL)	Cytotoxicity (Vero) TC_{50} (μg/ml)	Anti-HIV-1		*Leishmania donovani*	
					EC_{50} (μM)	EC_{90} (μM)	IC_{50} (μg/mL)	IC_{90} (μg/mL)
2	—	1.1	0.4	—	0.6	—	0.7	1.1
3	>128	2.0	1.3	NC	1.3	8.0	1.7	2.7
4	>128	0.3	1.1	NC	0.5	3.0	0.1	0.2
5	>128	0.4	1.5	NC	10.9	33.5	1.3	2.5
6	>128	1.8	3.8	NC	37.7	70.6	4.1	9.5
7	>128	1.8	4.1	NC	2.1	10.5	1.4	2.5
8	>128	2.9	NA	NC	45.9	95.4	6.8	12.0
9	>128	3.3	3.7	NC	4.6	33.9	1.7	2.7
10	>128	0.6	0.9	NC	4.0	25.2	1.6	2.7
11	>128	0.4	0.8	NC	9.9	30.6	1.8	5.5
12	>128	0.6	2.5	NC	2.3	16.3	1.8	5.0
13	>128	0.3	1.2	NC	3.8	7.1	1.5	2.5
14	>128	0.4	1.3	NC	18.8	66.4	1.4	2.6
15	>128	0.4	1.1	NC	16.6	54.3	6.0	11.0
16	>128	0.2	1.0	NC	9.2	29.1	1.6	2.6
17	>128	0.2	1.0	NC	3.7	6.9	0.4	0.7
18	>128	3.0	NA	NC	>100	>100	26.0	42.0
19	>128	3.0	4.3	NC	52.8	>100	6.2	12.0
20	>128	0.8	1.5	NC	8.2	25.3	4.8	10.0
21	41.03	0.3	0.8	NC	33.7	60.1	4.3	9.5
Pentamidine	—	—	—	—	—	—	1.6	3.5
Amphotericin B	—	—	—	—	—	—	1.1	2.3
Chlorquine	—	0.0165	0.140	—	—	—	—	—

IC_{50} and IC_{90} are the sample concentrations that kill 50% and 90% cells compared to the solvent controls. For malarial assays, screens were run at 4760, 1587, and 528.8 ng/mL. For *Leishmania* assays, screens were run at 50, 12.5, and 3.125 μg/mL NA, not active; NT, not tested: NC, not cytotoxic (4.7 μg/mL).

Compound **19**, deviating from the aforementioned pattern, consists of a 17 carbon acyl ester chain with an unsaturation between C9′ and C10′.

Tuberculosis, malaria, and *leishmaniasis*. Isoaaptamine (**2**) did not show activity against *Mycobacterium tuberculosis*. However, the derivative (**21**) was active with IC_{50} values of 41.03 μg/mL. There was no evident congruence in the derivative structure and the activity reported.

The activity of isoaaptamine (**2**, IC_{50} 0.68 μg/mL) was more active than both pentamidine (IC_{50} 1.6 μg/mL) and amphotericin B (IC_{50} 1.1 μg/mL) against *Leishmania donovani*. Modification of isoaaptamine (**2**) resulted in an increase in activity with the most active derivative **4** (IC_{50} 0.1 μg/mL) containing a para ethyl-substituted phenyl ring and **17** (IC_{50} 0.4 μg/mL) containing a para *tert*-butyl-substituted phenyl ring. Substitution of a group longer than two carbons in the para position decreases the activity against *Leishmania*. Isoaaptamine (**2**) shows remarkable activity against the W2 clone and mild activity against the D6 clone of *P. falciparum* prior to modification (380, 1100 ng/mL, respectively). All modifications had a negative impact on the activity against the W2 clone. However, an increase in D6 activity of many of the derivatives was observed (**4**, **5**, **10**–**17**, **20**, and **21**) with para substitution on the phenyl ring of short carbon chains for compounds **4** (IC_{50} 330 ng/mL), **16** (IC_{50} 230 ng/mL), and **17** (IC_{50} 240 ng/mL) being the most potent. A decrease in activity corresponding to extension of the chain was also observed. Although additional derivatives showed activity, no other obvious patterns were evident.

2.3. Cancer cell cytotoxicity

Isoaaptamine (**2**) has shown remarkable activity against a range of different cancer cell lines with activity against the murine leukemia cell line P388 as low as 0.28 μg/mL.[6] All 21 compounds were evaluated against 14 different cancer cell lines, many of which can be found in Table 4. The compounds found to have broad activity against the tested cell lines (**4**, **10**, **12**–**14**, **16**, **17**, **19**, and **20**) contained para substituted phenyl rings. Most notable were the activities of **13** (GI_{50} 1.66 μM), **14** (GI_{50} 0.05 μM), and **17** (GI_{50} 1.9 μM) against the leukemia cell line K-562. Compound **14** was substituted with a 5 carbon chain at the para position while compounds **13** and **17** were substituted with a 4 carbon chain and a *t*-butyl group, respectively. A decrease in activity was observed with a methyl (**16**, 5.8 μM) or an ethyl (**4**, 6.0 μM) substituent at the para position.

The prevalence of para substitution of a phenyl ring attached via an ester linkage to the C9 hydroxyl position of isoaaptamine (**2**) appears to be the underlying SAR evident in the data presented in this paper. The substituent at the para position determined the selectivity toward the target of interest. Substitution of a phenyl ester moiety at the C9 position of isoaaptamine (**2**) was more effective than the acylation previously

Table 4. Anti-cancer data

1° Screening		Prostate DU-145 (μM)	Ovary IGROV-ET (μM)	Breast SK-BR3 (μM)	Melanoma SK-MEL-28 (μM)	Lung A549 (μM)	Leukemia K-562 (μM)	Pancreas PANC1 (μM)	Colon LOVO (μM)	Cervix HELA-APL (μM)
3	GI_{50}	>28.9	13.8	>28.9	15.9	>28.9	15.0	8.5	10.4	14.3
	TGI	>28.9	>28.9	>28.9	>28.9	>28.9	20.2	24.3	28.9	>28.9
	LC_{50}	>28.9	>28.9	>28.9	>28.9	>28.9	27.0	28.9	>28.9	>28.9
4	GI_{50}	5.4	4.1	7.3	5.3	5.5	6.0	3.2	4.3	4.8
	TGI	9.2	8.4	14.4	9.1	9.5	9.6	6.6	8.3	8.9
	LC_{50}	15.8	17.1	17.8	15.5	16.5	15.3	13.4	16.3	16.5
5	GI_{50}	13.5	9.6	9.4	7.5	9.6	10.0	4.8	5.1	6.9
	TGI	>28.5	>28.5	20.8	23.2	25.2	14.3	9.3	11.9	17.9
	LC_{50}	>28.5	>28.5	>28.5	>28.5	>28.5	20.3	18.3	27.6	>28.5
6	GI_{50}	15.8	10.7	9.3	4.8	12.2	7.1	5.1	4.9	10.0
	TGI	>27.1	>27.1	18.3	9.1	>27.1	11.0	10.8	11.4	27.1
	LC_{50}	>27.1	>27.1	>27.1	17.1	>27.1	17.1	23.1	26.4	>27.1
7	GI_{50}	6.9	5.7	6.2	4.9	6.1	8.8	4.6	4.6	5.7
	TGI	15.0	10.0	11.0	8.4	12.5	12.5	8.3	8.3	10.8
	LC_{50}	>27.1	17.4	19.5	14.3	25.4	17.9	15.0	14.9	20.2
8	GI_{50}	>30.5	25.7	>30.5	29.4	>30.5	26.5	14.1	18.1	30.5
	TGI	>30.5	>30.5	>30.5	>30.5	>30.5	>30.5	>30.5	>30.5	>30.5
	LC_{50}	>30.5	>30.5	>30.5	>30.5	>30.5	>30.5	>30.5	>30.5	>30.5
9	GI_{50}	8.3	9.2	10.4	5.6	9.6	7.9	5.4	7.5	6.8
	TGI	18.9	18.2	>26.4	9.5	26.4	11.8	9.3	15.2	12.4
	LC_{50}	>26.4	>26.4	>26.4	16.2	>26.4	17.9	16.0	>26.4	22.7
10	GI_{50}	4.8	3.4	5.0	5.0	5.0	6.4	2.8	3.5	4.5
	TGI	8.4	6.8	8.6	8.7	9.0	10.0	6.1	7.0	8.3
	LC_{50}	14.7	13.8	14.8	15.1	16.2	15.6	13.0	13.8	15.2
11	GI_{50}	14.8	10.8	15.8	9.8	>28.9	8.1	5.3	7.9	6.6
	TGI	>28.9	>28.9	>28.9	28.9	>28.9	13.4	9.9	17.6	14.0
	LC_{50}	>28.9	>28.9	>28.9	>28.9	>28.9	22.2	18.4	>28.9	28.9
12	GI_{50}	5.6	4.4	11.3	4.2	11.9	2.8	3.1	3.0	3.8
	TGI	14,1	9.0	24.0	7.9	>24.0	5.6	6.3	6.2	8.3
	LC_{50}	>24.0	18.3	>24.0	15.0	>24.0	11.0	12.9	12.8	17.8
13	GI_{50}	4.4	8.1	7.3	3.9	4.7	**1.7**	2.8	2.9	3.6
	TGI	8.0	12.0	11.2	7.4	8.3	4.3	5.9	5.9	7.0
	LC_{50}	14.4	17.8	17.3	14.0	14.5	9.8	12.4	12.2	13.6
14	GI_{50}	3.8	2.9	6.5	3.0	4.5	**0.1**	1.1	**1.5**	**1.0**
	TGI	7.6	6.1	10.1	6.0	8.0	0.5	3.7	4.5	3.3
	LC_{50}	15.5	12.6	15.8	12.0	14.3	1.1	9.6	10.8	9.2
15	GI_{50}	>27.1	16.2	21.9	10.5	27.1	3.6	6.0	9.4	13.9
	TGI	>27.1	>27.1	>27.1	27.1	>27.1	7.5	13.4	27.1	>27.1
	LC_{50}	>27.1	>27.1	>27.1	>27.1	>27.1	15.5	>27.1	>27.1	>27.1
16	GI_{50}	6.2	5.8	6.5	4.9	5.8	5.8	3.8	3.4	4.8
	TGI	10.7	10.5	10.7	8.8	10.8	9.6	7.6	6.9	8.9
	LC_{50}	18.6	18.9	17.8	15.6	20.3	15.9	14.8	14.0	16.6
17	GI_{50}	4.9	4.3	5.8	4.8	4.9	**1.9**	2.8	3.2	4.7
	TGI	8.7	7.9	9.5	8.4	8.6	4.2	6.0	6.5	8.2
	LC_{50}	15.0	14.6	15.5	14.5	15.0	9.6	12.4	13.1	14.4
18	GI_{50}	>30.7	23.2	>30.7	27.0	28.2	>30.7	16.8	12.3	30.7
	TGI	>30.7	>30.7	>30.7	>30.7	>30.7	>30.7	>30.7	>30.7	>30.7
	LC_{50}	>30.7	>30.7	>30.7	>30.7	>30.7	>30.7	>30.7	>30.7	>30.7

(*continued on next page*)

Table 4 (*continued*)

1° Screening		Prostate DU-145 (μM)	Ovary IGROV-ET (μM)	Breast SK-BR3 (μM)	Melanoma SK-MEL-28 (μM)	Lung A549 (μM)	Leukemia K-562 (μM)	Pancreas PANC1 (μM)	Colon LOVO (μM)	Cervix HELA-APL (μM)
19	GI_{50}	3.6	9.1	5.6	3.7	7.4	5.7	3.1	3.2	3.6
	TGI	6.4	>20.3	10.2	6.5	20.3	8.6	5.8	5.9	6.6
	LC_{50}	11.3	>20.3	18.4	11.4	>20.3	13.0	10.8	10.9	11.9
20	GI_{50}	9.1	4.9	6.9	4.8	6.1	4.4	4.4	4.5	4.9
	TGI	24.3	8.9	12.1	8.7	10.9	8.0	8.3	8.1	8.9
	LC_{50}	>28.0	16.2	21.1	15.5	19.3	14.6	15.6	14.6	16.3
21	GI_{50}	19.5	11.0	>27.6	6.1	20.8	6.7	5.2	5.0	5.7
	TGI	>27.6	25.6	>27.6	11.5	>27.6	12.6	10.5	9.4	10.4
	LC_{50}	>27.6	>27.6	>27.6	21.6	>27.6	23.8	21.2	17.7	18.9

GI_{50} is the concentration at which 50% growth inhibition was observed. TGI is the concentration at which total growth inhibition was observed. LC_{50} is the lethal concentration at which 50% cell death occurred.

reported at this position by Shen et al. A further point of observation reveals the congruence of the attachment of para substituted cyclic moieties in this group of compounds with and overall increase in activity. This observation reflects the results found in the present study and those previously published by Pettit et al.

In conclusion, this is the first reported SAR investigation for anti-HIV-1 activity of the aaptamine alkaloids thus far. In addition, we are now able to report several optimized potential antitumor (**12**–**14**, and **17**) and anti-infective leads (**4**, **13**, **14**, **17**, and **19**), suggesting that further investigations of this class of marine natural products maybe fruitful. Natural products have been credited with as many as 75% of the treatments of infectious diseases and 60% of treatments for cancer.[23] However only 5–6% represent the unmodified natural product indicating the importance of optimizing novel marine natural product structural classes with reasonable drug-like properties.

3. Experimental

3.1. General

1D and 2D NMR spectra were recorded on a Bruker Avance DRX-400 spectrometer. Chemical shift (δ) values expressed in parts per million (ppm) are referenced to the residual solvent signals with resonances at δ_H/δ_C 7.26/77.00 ($CDCl_3$). ESI-FTMS analyses were measured on a Bruker-Magnex BioAPEX 30es ion cyclotron HR HPLC-FT spectrometer by direct injection into an electrospray interface. TLC was performed on aluminum sheets (Si gel 60 F_{254}, Merck KGaA, Germany) with an acetone/hexane (80:20) sol-

Table 5. ^1H and ^{13}C NMR spectral data for compounds **3**, **4**, and **5**

Position	**3**		**4**		**5**	
	δ_H	δ_C	δ_H	δ_C	δ_H	δ_C
2	6.9, br d	133.6, d	7.2, d(7.6)	130.1, d	6.9, d(6.8)	133.2, d
3	6.8, br d	100.9, d	6.4, d(7.2)	101.5, d	6.8, br d	113.3, d
3a		148.9, s		151.9, s		146.1, s
5	7.5, br d	147.2, d	7.9, d(7.2)	148.1, d	7.5, d(6.4)	146.1, d
6	7.3, br d	113.5, d	7.7, d(7.2)	113.6, d	7.5, d(6.4)	116.4, d
6a		136.3, s		136.4, s		136.6, s
7	6.8, br s	100.3, d	7.0, s	98.8, d	6.8, s	99.9, d
8		157.2, s		157.9, s		156.7, s
9		126.9, s		124.4, s		134.7, s
9a		124.0, s		127.3, s		124.3, s
9b		117.8, s		117.6, s		117.9, s
NCH_3	3.8, s	45.4, q	4.0, s	44.8, q	3.9, s	45.0, q
OCH_3	3.9, s	56.8, q	3.9, s	56.2, q	3.9, s	56.6, q
1′		165.4, s		164.9, s		164.0, s
2′		134.9, s		125.6, s		123.3, s
3′		141.9, s	8.1, d(8)	130.4, d	8.2, br d	133.1, d
4′	7.1, br d	130.9,d	7.46, d(8)	128.3, d	7.2, br d	114.5, d
5′	7.5, br d	132.2, d		149.1, s		167.8, s
6′	7.3, br d	126.3, d	7.46, d(8)	128.3, d	7.2, br d	114.5, d
7′	8.1, d(7.6)	131.5, d	8.1, d(8)	130.4, d	8.2, br d	133.1, d
8′	2.6, s	21.8, q	2.7, q(7.6)	28.6, t		F
9′			1.3, t(7.6)	14.3, t		

Measured in $CDCl_3$ at 400 MHz for ^1H and 100 MHz for ^{13}C, respectively. *J* values in Hz.

vent system. All acyl halides were purchased from Sigma–Aldrich, USA.

Isoaaptamine (**2**) (150 mg, 0.657 mmol) was dissolved in dry methylene chloride (2 mL) at 0 °C, 0.5 mL of tri-ethyl amine was added, and the reaction mixture was stirred for 30 min. An excess of the acyl halide was added dropwise over a period of 15 min. The reaction was allowed to stir at 0 °C for 30 min, slowly warmed to room temperature, and the progress was monitored on TLC. The reaction was stopped when the TLC showed the reaction was completed (2–24 h). The residue was fractionated on silica gel G254 2000 μm using MeOH/$CHCl_3$ (80:20) and yielded products of various colors for compounds **3**–**21**.

3.1.1. 9-*O*-2-methylbenzoylisoaaptamine (3). Brownish amorphous solid; ^1H and ^{13}C NMR ($CDCl_3$) data see

Table 6. ^1H and ^{13}C NMR spectral data for compounds **6**, **7**, and **8**

Position	6		7		8	
	δ_H	δ_C	δ_H	δ_C	δ_H	δ_C
2	7.5, d(8)	124.6, d	7.3, br d	123.0, d	7.3, br d	130.0, d
3	6.8, br d	113.5, d	5.3, br d	113.5, d	6.7, br d	101.1, d
3a		149.0, s		156.7, s		148.7, s
5	7.9, br d	127.5, d	7.0, br d	123.3, d	7.6, d(5.2)	147.4, d
6	7.3, br d	118.3, d	6.8, br d	118.9, d	6.9, d(5.2)	113.3, d
6a		136.8, s		148.9, s		135.7, s
7	6.8, s	100.5, d	6.8, s	100.6, d	6.8, s	99.7, d
8		156.7, s		156.9, s		153.8, s
9		134.6, s		136.6, s		135.0, s
9a		118.5, s		134.4, s		125.1, s
9b		100.9, s		118.2, s		117.6, s
NCH_3	3.9, s	45.2, q	3.9, s	45.1, q	3.9, s	45.3, q
OCH_3	3.9, s	56.8, q	3.8, s	56.8, q	3.9, s	56.8, q
1′		161.7, s		161.6, s		42.7, t
2′		117.7, s		118.7, d	3.4, br q	14.1, q
3′	7.9, br d	123.2, d	7.8, s	157.1, ,s	1.2, t(6.8)	42.3, t
4′	7.0, br t	123.1, d		119.1, d	3.4, br q	13.3, q
5′	7.1, br d	118.4, d	7.0, br d	117.5, d	1.3, t(6.8)	
6′		146.6, s	7.0, br d	158.8, s		
7′		149.9, s		N		

Measured in $CDCl_3$ at 400 MHz for ^1H and 100 MHz for ^{13}C, respectively. *J* values in Hz.

Table 7. ^1H and ^{13}C NMR spectral data for compounds **9**, **10**, and **11**

Position	9		10		11	
	δ_H	δ_C	δ_H	δ_C	δ_H	δ_C
2	7.3, d(7.2)	128.8, d	7.4, d(7)	128.6, d	6.7, br d	131.8, d
3	7.3, br d	113.4, d	6.8, d(7)	101.1, d	6.5, br d	101.1, d
3a		148.8, s		148.7, s		148.7, s
5	7.5, d(7.6)	128.9, d	7.6, br d	130.1, d	7.3, br d	147.7, d
6	7.3, br d	125.2, d	7.1, d(6)	113.5, d	7.3, br d	113.5, d
6a		134.9, s		136.4, s		136.2, s
7	6.7, s	101.3, d	6.8, s	100.1, d	6.8, s	100.1, d
8		157.2, s		157.3, s		157.0, s
9		134.3, s		134.8, s		134.6, s
9a		126.5, s		123.9, s		123.8, s
9b		117.7, s		117.6, s		117.5, s
NCH_3	3.7, s	44.7, q	3.9, s	45.6, q	3.7, s	45.5, q
OCH_3	3.9, s	56.1, q	3.9, s	56.9, q	3.7, s	57.0, q
1′	4.0, s	168.3, s		164.4, s		165.0, s
2′		46.4, t		127.8, s		127.9, s
3′	7.3, br d	136.3, s	8.2, d(8)	130.9, d	7.8, br d	127.7, d
4′	7.2, br t	128.5, d	7.6, d(8)	129.1, d	7.4, br t	128.9, d
5′	7.1, t(6.8)	128.7, d		144.0, s	7.4, br d	135.2, d
6′	7.2, br t	127.7, d	7.6, d(8)	129.1, d		138.9, s
7′	7.3, br d	128.7, d	8.2 d(8)	130.9, d	7.8, s	131.0, d
8′		128.4, d	4.7, s	45.2, t	2.3, s	21.2, q
9′				Cl		

Measured in $CDCl_3$ at 400 MHz for ^1H and 100 MHz for ^{13}C, respectively. *J* values in Hz.

Table 8. ^{1}H and ^{13}C NMR spectral data for compounds **12**, **13**, and **14**

Position	**12**		**13**		**14**	
	δ_H	δ_C	δ_H	δ_C	δ_H	δ_C
2	7.2, br d	119.8, d	7.0, d(5.6)	127.8, d	7.0, d(7.2)	131.8, d
3	6.8, br d	100.6, d	6.8, d(5.6)	103.5, d	6.8, br d	113.4, d
3a		136.6, s		150.8, s		150.3, s
5	7.5, br d	131.6, d	8.0, br d	144.4, d	7.5, d(6.8)	147.1, d
6	7.5, br d	113.5, d	7.2, d(6.8)	113.4, d	7.4, br d	127.8, d
6a		126.3, s		136.8, s		136.1, s
7	6.8, s	100.6, d	6.6, s	98.6, d	6.8, s	100.7, d
8		153.7, s		156.2, s		156.9, s
9		134.9, s		134.9, s		134.5, s
9a		118.9, s		123.0, s		123.6, s
9b		117.9, s		118.8, s		117.5, s
NCH_3	3.9, s	45.5, q	3.7, s	44.7, q	3.9, s	45.3, q
OCH_3	3.9, s	56.8, q	3.8, s	56.4, q	3.9, s	56.8, q
1′		157.1, s		165.2, s		164.9, s
2′		123.7, s		125.8, s		125.4, s
3′	8.2, d(6.8)	132.7, d	8.1, d(8)	130.6, d	8.1, d(7.6)	130.6, d
4′	7.4, d(7.2)	120.7, d	7.3, d(8)	129.0, d	7.3, br d	129.0, d
5′		163.8, s		150.1, s		148.9, s
6′	7.4, d(7.2)	120.7, d	7.3, d(8)	129.0, d	7.3, br d	129.0, d
7′	8.2, d(6.8)	132.7, d	8.1, d(8)	130.6, d	8.1, d(7.6)	130.6, d
8′			2.7, t(7.6)	35.8, t	2.7, t(8)	36.0, t
9′			1.6, m(7.6)	33.2, t	1.7, br m	31.4, t
10′			1.4, m(7.6)	22.3, t	1.3, br m	30.7, t
11′			0.9, t(7.6)	13.9, q	1.3, br m	22.4, t
12′					0.9, br t	13.9, t

Measured in $CDCl_3$ at 400 MHz for ^{1}H and 100 MHz for ^{13}C, respectively. *J* values in Hz.

Table 9. ^{1}H and ^{13}C NMR spectral data for compounds **15**, **16**, and **17**

Position	**15**		**16**		**17**	
	δ_H	δ_C	δ_H	δ_C	δ_H	δ_C
2	7.1, br d	131.4, d	6.9, d(6)	132.1, d	7.0, br d	131.5, d
3	6.8, br d	101.0, d	6.8, d(6)	101.2, d	6.8, br d	113.4, d
3a		149.2, s		149.4, s		149.2, s
5	7.6, d(6)	147.0, d	8.0, d(7.6)	146.4, d	7.5, br d	147.0, d
6	7.5, br d	118.3, d	7.2, d(7.6)	113.4, d	7.5, br d	124.8, d
6a		136.7, s		135.5, s		136.5, s
7	6.8, s	101.0, d	6.7, s	101.1, d	6.8, s	100.7, d
8		151.6, s		157.2, s		158.5, s
9		135.0, s		135.0, s		135.0, s
9a		123.8, s		123.9, s		124.0, s
9b		117.9, s		118.1, s		118.0, s
NCH_3	3.9, s	45.3, q	3.8, s	45.4, q	3.9, s	45.5, q
OCH_3	3.9, s	56.8, q	3.9, s	56.7, q	3.9, s	56.8, q
1′		163.2, s		164.9, s		164.9, s
2′		125.0, s		125.3, s		125.2, s
3′	8.0, br d	127.8, d	8.1, d(8)	130.5, d	8.1, d(8)	130.5, d
4′	7.4, dd(8)	113.6, d	7.3, d(8)	129.7, d	7.6, d(8)	126.0, d
5′		157.2, s		145.5, s		157.3, s
6′		149.0, s	7.3, d(8)	129.7, d	7.6, d(8)	126.0, d
7′	8.0, br d	118.1, d	8.1, d(8)	130.5, d	8.1, d(8)	130.5, d
8′			2.5, s	21.8, q		35.3, s
9′					1.4, s	31.0, q
10′					1.4, s	31.0, q
11′					1.4, s	31.0, q

Measured in $CDCl_3$ at 400 MHz for ^{1}H and 100 MHz for ^{13}C, respectively. *J* values in Hz.

Table 5; ESI-MS *m/z* 347 (M^+, 100). High resolution EI-MS calculated for $C_{21}H_{18}N_2O_3$ (M^+) *m/z* 347.1396, observed *m/z* 347.1396.

3.1.2. 9-*O*-4-ethylbenzoylisoaaptamine (4). Brownish powder; ^1H and ^{13}C NMR ($CDCl_3$) data see Table 5; ESI-MS *m/z* 361 (M^+, 100). High resolution EI-MS calculated for $C_{22}H_{20}N_2O_3$ (M^+) *m/z* 361.1552, observed *m/z* 361.1551.

3.1.3. 9-*O*-4-fluorobenzoylisoaaptamine (5). Yellow amorphous solid; ^1H and ^{13}C NMR ($CDCl_3$) data see Table 5; ESI-MS *m/z* 351 (M^+, 100). High resolution EI-MS calculated for $C_{20}H_{15}N_2O_3F$ (M^+) *m/z* 351.1145, observed *m/z* 351.1145.

3.1.4. 9-*O*-2,3-difluorobenzoylisoaaptamine (6). Brownish amorphous solid; ^1H and ^{13}C NMR ($CDCl_3$) data see Table 6; ESI-MS *m/z* 369 (M^+, 100). High resolution EI-MS calculated for $C_{20}H_{14}N_2O_3F_2$ (M^+) *m/z* 369.1051, observed *m/z* 369.1059.

3.1.5. 9-*O*-2,5-difluorobenzoylisoaaptamine (7). Reddish brown amorphous solid; ^1H and ^{13}C NMR ($CDCl_3$) data see Table 6; ESI-MS *m/z* 369 (M^+, 100). High resolution EI-MS calculated for $C_{20}H_{14}N_2O_3F_2$ (M^+) *m/z* 369.1051, observed *m/z* 369.1054.

3.1.6. 9-*O*-diethylcarbamoylisoaaptamine (8). Dark red amorphous solid; ^1H and ^{13}C NMR ($CDCl_3$) data see Table 6; ESI-MS *m/z* 328 (M^+, 100). High resolution EI-MS calculated for $C_{18}H_{21}N_3O_3$ (M^+) *m/z* 328.1661, observed *m/z* 328.1653.

3.1.7. 9-*O*-2-(thiophenyl)acetylisoaaptamine (9). Greenish black amorphous solid; ^1H and ^{13}C NMR ($CDCl_3$) data see Table 7; ESI-MS *m/z* 379 (M^+, 100). High resolution EI-MS calculated for $C_{21}H_{18}N_2O_3S$ (M^+) *m/z* 379.1116, observed *m/z* 379.1113.

3.1.8. 9-*O*-4-chloromethylbenzoyl isoaaptamine (10). Dark yellow amorphous solid; ^1H and ^{13}C NMR ($CDCl_3$) data see Table 7; ESI-MS *m/z* 381 (M^+, 100). High resolution EI-MS calculated for $C_{21}H_{17}N_2O_3Cl$ (M^+) *m/z* 381.1006, observed *m/z* 381.1000.

3.1.9. 9-*O*-3-methylbenzoylisoaaptamine (11). Brown amorphous solid; ^1H and ^{13}C NMR ($CDCl_3$) data see Table 7; ESI-MS *m/z* 347 (M^+, 100). High resolution EI-MS calculated for $C_{21}H_{18}N_2O_3$ (M^+) *m/z* 347.1396, observed *m/z* 347.1391.

3.1.10. 9-*O*-4-trifluoromethoxybenzoylisoaaptamine (12). Yellowish brown amorphous solid; ^1H and ^{13}C NMR

Table 10. ^1H and ^{13}C NMR spectral data for compounds **18**, **19**, and **20**

Position	18		19		20	
	δ_H	δ_C	δ_H	δ_C	δ_H	δ_C
2	6.9, d(6.8)	130.0, d	7.4, d(7.2)	130.0, d	7.8, d(6.4)	131.7, d
3	6.7, d(6.8)	101.2, d	7.1, d(7.2)	113.3, d	6.8, d(6.4)	113.6, d
3a		148.5, s		148.8, s		150.5, s
5	7.6, d(7.2)	147.6, d	7.5, d(6.8)	147.2, d	7.7, d(7.6)	144.7, d
6	7.3, br d	113.3, d	6.8, br d	129.6, d	7.0, d(7.6)	129.9, d
6a		135.6, s		136.0, s		135.0, s
7	6.8, s	99.6, d	6.8, s	100.6, d	6.7, s	99.1, d
8		152.6, s		156.7, s		156.1, s
9		134.8, s		123.7, s		132.1, s
9a		124.8, s		134.3, s		122.8, s
9b		117.4, s		117.5, s		117.6, s
NCH_3	3.9. s	45.5, q	4.0, s	45.2, q	3.7, s	44.8, q
OCH_3	3.9, s	57.0, q	3.9, s	56.7, q	3.9, s	56.6, q
1′		158.0, s		172.0, s		163.7, s
2′	3.5, br t	46.9, t	2.6, t(7.2)	33.9, t		137.2, s
3′	2.0, br m	24.9, t	1.8, br m	24.6, t	8.3, d(8)	131.0, d
4′	2.0, br m	25.8, t	1.3, br m	29.0, t	7.9, d(8)	132.8, d
5′	3.5, br t	46.8, t	1.3, br m	29.2, t		118.7, s
6′			1.3, br m	29.7, t	7.9, d(8)	132.8, d
7′			1.3, br m	29.2, t	8.3, d(8)	131.0, d
8′			2.0, br q	27.1, t		117.7, s
9′			5.4, br q	129.7, d		
10′			5.4, br q	129.8, d		
11′			2.0, br q	27.1, t		
12′			1.3, br m	29.2, t		
13′			1.3, br m	29.4, t		
14′			1.3, br m	29.6, t		
15′			1.3, br m	29.1, t		
16′			1.3, br m	31.8, t		
17′			1.3, br m	22.6, t		
18′			0.9, br t	14.1, q		

Measured in $CDCl_3$ at 400 MHz for ^1H and 100 MHz for ^{13}C, respectively. *J* values in Hz.

($CDCl_3$) data see Table 8; ESI-MS *m/z* 417 (M^+, 100). High resolution EI-MS calculated for $C_{21}H_{15}N_2O_4F_3$ (M^+) *m/z* 417.1062, observed *m/z* 417.1069.

3.1.11. 9-*O*-4-butylbenzoylisoaaptamine (13). Brown amorphous solid; ^1H and ^{13}C NMR ($CDCl_3$) data see Table 8; ESI-MS *m/z* 389 (M^+, 100). High resolution EI-MS calculated for $C_{24}H_{24}N_2O_3$ (M^+) *m/z* 389.1865, observed *m/z* 389.1875.

3.1.12. 9-*O*-4-pentylbenzoylisoaaptamine (14). Brown amorphous solid; ^1H and ^{13}C NMR ($CDCl_3$) data see Table 8; ESI-MS *m/z* 403 (M^+, 100). High resolution EI-MS calculated for $C_{25}H_{26}N_2O_3$ (M^+) *m/z* 403.2022, observed *m/z* 403.2009.

3.1.13. 9-*O*-3,4-difluorobenzoylisoaaptamine (15). Greenish powder; ^1H and ^{13}C NMR ($CDCl_3$) data see Table 9; ESI-MS *m/z* 369 (M^+, 100). High resolution EI-MS calculated for $C_{20}H_{14}N_2O_3F_2$ (M^+) *m/z* 369.1051, observed *m/z* 369.1065.

3.1.14. 9-*O*-4-methylbenzoylisoaaptamine (16). Brown amorphous solid; ^1H and ^{13}C NMR ($CDCl_3$) data see Table 9; ESI-MS *m/z* 347 (M^+, 100). High resolution EI-MS calculated for $C_{21}H_{18}N_2O_3$ (M^+) *m/z* 347.1396, observed *m/z* 347.1378.

3.1.15. 9-*O*-4-*tert*-butylbenzoylisoaaptamine (17). brown amorphous solid; ^1H and ^{13}C NMR ($CDCl_3$) data see Table 9; ESI-MS *m/z* 389 (M^+, 100). High resolution EI-MS calculated for $C_{24}H_{24}N_2O_3$ (M^+) *m/z* 389.1865, observed *m/z* 389.1877.

3.1.16. 9-*O*-1-(pyrrolidine)carbonylisoaaptamine (18). Pale orange oil; ^1H and ^{13}C NMR ($CDCl_3$) data see Table 10; ESI-MS *m/z* 326 (M^+, 100). High resolution EI-MS calculated for $C_{18}H_{19}N_3O_3$ (M^+) *m/z* 326.1505, observed *m/z* 326.1501.

3.1.17. 9-*O*-*Z*-oleoylisoaaptamine (19). Brown amorphous solid; ^1H and ^{13}C NMR ($CDCl_3$) data see Table 10; ESI-MS *m/z* 493 (M^+, 100). High resolution EI-MS calculated for $C_{31}H_{44}N_2O_3$ (M^+) *m/z* 493.3430, observed *m/z* 493.3412.

3.1.18. 9-*O*-4-cyanobenzoylisoaaptamine (20). Brownish amorphous solid; ^1H and ^{13}C NMR ($CDCl_3$) data see Table 10; ESI-MS *m/z* 358 (M^+, 100). High resolution EI-MS calculated for $C_{21}H_{15}N_3O_3$ (M^+) *m/z* 358.1192, observed *m/z* 358.1192.

3.1.19. 9-*O*-3-methoxybenzoylisoaaptamine (21). Brown amorphous solid; ^1H and ^{13}C NMR ($CDCl_3$) data see Table 11; ESI-MS *m/z* 363 (M^+, 100). High resolution EI-MS calculated for $C_{21}H_{18}N_2O_4$ (M^+) *m/z* 363.1219, observed *m/z* 363.1224.

Table 11. ^1H and ^{13}C NMR spectral data for compound **21**

Position	21	
	δ_H	δ_C
2	7.1, br d	131.4, d
3	6.8, br d	100.8, d
3a		148.9, s
5	7.8, d(7.6)	147.1, d
6	7.4, br d	115.0, d
6a		136.4, s
7	6.8, s	100.6, d
8		157.1, s
9		129.2, s
9a		123.8, s
9b		117.7, s
NCH_3	3.9, s	45.5, q
OCH_3	3.9, s	56.9, q
1′		164.8, s
2′		134.8, s
3′	7.7, s	113.4, d
4′		159.9, s
5′	7.1, br d	120.7, d
6′	7.5, t(8.4)	130.1, d
7′	7.5, br d	122.8, d
8′	3.9, s	55.6, q

Measured in $CDCl_3$ at 400 MHz for ^1H and 100 MHz for ^{13}C, respectively. *J* values in Hz.

Acknowledgments

We are indebted to S. Wahyuono and A. Mursyidi from Gadjah Mada University, Indonesia, for assistance with sample collection, J. Trott for in vitro malaria assays, B. Tekwani for leishmania assays, S. Franzblau and F. Zhang for Mtb assays, and P. Tharnish for anti-HIV-1 assays. We are also indebted to S. Sanders and B. Smiley, from the National Center for Natural Products Research, for bioassays. We are grateful to A. Holley, A. Murphy, and J. Fiechtl for their help in table preparation and J. Mustafa for valuable suggestions and discussions. This work was supported by NIH (R01A136596, KO2AI01502), PharmaMar, R.F.S. is supported by the Emory University Center for AIDS Research and Department of Veterans Affairs. This investigation was conducted in a facility constructed with support from Research Facilities Improvement Program (C06 RR-14-503-01) from the National Center for Research Resources (NIH).

Supplementary data

Supplementary data associated with this article can be found, in the online version, at doi:10.1016/j.bmc.2006.08.042.

References and notes

1. Nakamura, H.; Kobayash, J.; Ohizumi, Y.; Hirata, Y. *Tetrahedron Lett.* **1982**, *23*, 5555–5558.
2. Ohizumi, Y.; Kajiwara, A.; Nakamura, H.; Kobayashi, J. *J. Pharm. Pharmacol.* **1984**, *36*, 785–786.
3. Fedoreev, S.; Prokofeva, N.; Denisenko, V.; Rebachuk, N. *Khim. Farm. Zh.* **1988**, *22*, 943.
4. Kashman, Y.; Rudi, A.; Hirsh, S.; Isaacs, S.; Green, D.; Blasberger, D.; Carmely, S. *New J. Chem.* **1990**, *14*, 729–740.
5. Shen, Y.; Chein, C.; Hsieh, P.; Duh, C. *Taiwan Shuichan Xuehuikan* **1997**, *24*, 117.
6. Pettit, G. R.; Hoffmann, H.; McNulty, J.; Higgs, K. C.; Murphy, A.; Molloy, D. J.; Herald, D. L.; Williams, M.

D.; Pettit, R. K.; Doubek, D. L.; Hooper, J. N. A.; Albright, L.; Schmidt, J. M.; Chapuis, J.; Tackett, L. P. *J. Nat. Prod.* **2004**, *67*(3), 506–509.
7. Patil, A.; Westley, J.; Mattern, M.; Freyer, A.; Hofmann, G. PCT Int. Appl. WO 95/0584, March 1995.
8. Pettit, G. R.; Hoffmann, H.; Herald, D. L.; McNulty, J.; Murphy, A.; Higgs, K. C.; Hamel, E.; Lewin, N. E.; Pearce, L. V.; Blumberg, P. M.; Pettit, R. K.; Knight, J. C. *J. Org. Chem.* **2004**, *69*, 2251–2256.
9. Nitiss, J.; Zhou, J.; Rose, A.; Hsiung, Y.; Gale, K.; Osheroff, N. *Biochemistry* **1998**, *37*, 3078–3085.
10. O'Reilly, S.; Baker, S.; Sartorius, S.; Rowinsky, E.; Finizio, M.; Lubiniecki, G.; Grochow, L.; Gray, J.; Pieniaszek, H.; Donehower, R. *Ann. Oncol.* **1998**, *9*, 101–104.
11. Bousquet, P.; Brana, M.; Conlon, D.; Fitzgerald, K.; Perron, D.; Cocchiaro, C.; Miller, R.; Moran, M.; George, J.; Qian, X. *Cancer Res.* **1995**, *55*, 1176–1180.
12. Atwell, G.; Cain, B.; Baguley, B.; Finlay, G.; Denny, W. *J. Med. Chem.* **1984**, *27*, 1481–1485.
13. Denny, W.; Wakelin, L. *Cancer Res.* **1986**, *46*, 1719–1725.
14. Finlay, G.; Riou, J.; Baguley, B. *Eur. J. Cancer* **1996**, *32*, 708–714.
15. Hutchins, R.; Crenshaw, J.; Graves, D.; Denny, W. *Biochemistry* **2003**, *42*, 13754–13761.
16. Diers, J. A.; Pennaka, H. K.; Peng, J.; Bowling, J. J.; Duke, S. O.; Hamann, M. T. *J. Nat. Prod.* **2004**, *67*, 2117–2120.
17. Pettit, G. R.; Hoffmann, H.; Herald, D. L.; Blumberg, P. M.; Hamel, E.; Schmidt, J. M.; Chang, Y.; Pettit, R. K.; Lewin, N. E.; Pearce, L. V. *J. Med. Chem.* **2004**, *47*(7), 1775–1782.
18. Sugino, E.; Choshi, T.; Hibino, S. *Heterocycles* **1999**, *50*, 543.
19. Walz, A.; Sundberg, R. *J. Org. Chem.* **2000**, *65*, 8001.
20. Shen, Y. C.; Lin, T. T.; Sheu, J. H.; Duh, C. Y. *J. Nat. Prod.* **1999**, *62*, 1264–1267.
21. Gochfeld, D.; El Sayed, K.; Yousaf, M.; Hu, J.; Bartyzel, P.; Dunbar, D.; Wilkins, S.; Zjawiony, J.; Schinazi, R.; Wirtz, S.; Tharnish, P.; Hamann, M. *Mini Rev. Med. Chem.* **2003**, *3*, 401–424.
22. Wang, T.; Zhang, Z.; Wallace, O.; Deshpande, M.; Fang, H.; Yang, Z.; Zadjura, L.; Tweedie, D.; Huang, S.; Zhao, F.; Ranadive, S.; Robinson, B.; Gong, Y.; Ricarrdi, K.; Spicer, T.; Deminie, C.; Rose, R.; Wang, H.; Blair, W.; Shi, P.; Lin, P.; Colonno, R.; Meanwell, N. *J. Med. Chem.* **2003**, *46*, 4236–4423.
23. Newman, D. J.; Cragg, G. M.; Snader, K. M. *J. Nat. Prod.* **2003**, *66*, 1022–1037.